

RSC Advances



This is an *Accepted Manuscript*, which has been through the Royal Society of Chemistry peer review process and has been accepted for publication.

Accepted Manuscripts are published online shortly after acceptance, before technical editing, formatting and proof reading. Using this free service, authors can make their results available to the community, in citable form, before we publish the edited article. This *Accepted Manuscript* will be replaced by the edited, formatted and paginated article as soon as this is available.

You can find more information about *Accepted Manuscripts* in the [Information for Authors](#).

Please note that technical editing may introduce minor changes to the text and/or graphics, which may alter content. The journal's standard [Terms & Conditions](#) and the [Ethical guidelines](#) still apply. In no event shall the Royal Society of Chemistry be held responsible for any errors or omissions in this *Accepted Manuscript* or any consequences arising from the use of any information it contains.

ARTICLE

An investigation of physico-chemical properties of a new polyimide/silica composites

Cite this: DOI: 10.1039/x0xx00000x

T. AKhter^a, O. Ok Park^a, H. M. Siddiqi^b and S. Saeed^{c,d}, Khaled Mohammad Saoud^d

Received 00th January 2012,
Accepted 00th January 2012

DOI: 10.1039/x0xx00000x

www.rsc.org/

Abstract

A novel diamine 1,4-*bis*[4-(hydrazonomethyl)phenoxy]butane (4-BHPB) has been synthesized successfully by a facile method in the present study. 4-BHPB was reacted with pyromellitic dianhydride (PMDA) to derive a novel polyimide (PI). Highly compatibilized PI-SiO₂ nanocomposites were tailored using synthesized PI matrix and modified silica nanoparticles. The compatibility between organic-inorganic (O-I) components was improved remarkably by charge transfer complex (CTC) formed between PI chains and modified silica nanoparticles. PI chains have electron donor and acceptor groups (diamine and dianhydride portion respectively). These groups were generated in silica nanoparticles by the organic modification through 2,6-*bis*(3-(triethoxysilyl) propyl)pyrrolo[3,4-*f*]isoindole-1,3,5,7(2H,6H)-tetraone (M-SiO₂) which, in turn, was prepared reacting PMDA with 3-aminopropyltriethoxysilane. Sol-gel method was used for *in situ* synthesis of silica nanoparticles from a mixture of M-SiO₂ and TEOS. The enhanced compatibility between O-I phases through CTC formation furnished PI-SiO₂ nanocomposites (designated as OI-M) with improved thermal stability, hydrophobicity, and surface smoothness. For the comparison of properties, another series of PI-SiO₂ composites (OI-UM) were prepared dispersing unmodified silica micro-particles into PI matrix. OI-UM hybrid system does not contain CTC between PI matrix and silica particles. The structure of the monomer, PI, and organically modified silica network was analyzed by FTIR, and NMR spectroscopy. Thermogravimetric analysis, FE-SEM, contact angle measurement, and AFM were used to study thermal and morphological properties of synthesized PI-SiO₂ hybrids.

Introduction

Polyimides (PIs) have gained substantial importance as coating materials in microelectronics, aircraft, and electrical industries because they exhibit high mechanical and thermal stability, good optical properties, excellent resistance against organic solvents¹⁻⁴. However, certain applications like waveguide materials, spacecraft, electronics, and aircraft industries demand more improvements in hydrophobicity, thermal properties, and surface smoothness⁵. The properties and performance of PIs may be improved further by the addition of nano-scale silica into PI matrix giving organic-inorganic (O-I) hybrid materials⁶⁻⁹. O-I hybrids merge together the synergistic properties of PI matrix (ductility, and low temperature

processing) with low coefficient of thermal expansion and high thermal stability of silica nanoparticles¹⁰⁻¹². A number of techniques have been attempted for the preparation of O-I hybrid^{1, 2, 13}. Among these techniques, sol-gel reaction is most widely explored method for the preparation of O-I hybrids due to its versatility and provision of better control over surface morphology^{12, 14-17}. However, inorganic silicates and organic polymers behave differently during the condensation process of sol-gel reaction, consequently O-I phases are segregated from each other^{4, 18-20}. Properties of O-I composites are believed to be the outcome of interfacial interaction between matrix and filler phases²¹⁻²⁴. A number of research efforts are reported to avoid or at least minimize the phase separation between O-I components by adding different coupling agents^{12, 25-30}. Various

researchers studied the surface modification of silica particles to make them more compatible with organic matrix. Their studies demonstrated the improvement in the properties of O-I hybrid materials^{9, 15}. For instance, Musto *et al*¹⁰ explored the effect of controlled particle size and improved morphology on the properties of PI-SiO₂ composites prepared via sol-gel method by introducing γ -glycidoxypropyltrimethoxysilane as interphase coupling agent. Likewise, enhanced thermal and mechanical properties of O-I hybrids were achieved by Khalil *et al*³¹ using aminophenyltrimethoxysilane as a coupling agent owing to controlled particles size and uniform dispersion of nano-scale silica phase into PI matrix.

Many researches studied the tendency of PI chains to form charge transfer complex (CTC) with other polymer chains through their electron donor (diamine portion) and electron acceptor groups (dianhydride)³²⁻³⁴.

The present study reports the improvement of compatibility between polyimide matrix and silica nanoparticles through CTC. For this purpose a new diamine 1,4-*bis*[4-(hydrazonomethyl)phenoxy]butane (4-BHPB) was synthesized. 4-BHPB was subsequently reacted with pyromellitic dianhydride (PMDA) to prepare a novel PI. The PI chain inherently possesses electron donor groups (diamine portion) and electron acceptor groups (dianhydride portion). Existence of electron donor and acceptor groups in the reinforcement and thereby formation of CTC with PI chains was ensured by the organic modification of SiO₂ nanoparticles. Silica nanoparticles were synthesized using a mixture of TEOS and 2,6-*bis*(3-(triethoxysilyl)propyl)pyrrolo[3,4-*f*]isoindole-1,3, 5,7(2H,6H)-tetraone (M-SiO₂). M-SiO₂ was prepared by reacting APrTEOS with PMDA. Subsequently synthesized PI-SiO₂ nanocomposites (designated as OI-M) exhibited significantly improved thermal, morphological, and hydrophobic properties owing to enhanced phase connectivity between PI matrix and silica nanoparticles which is a direct consequence of CTC formed between O-I components. Moreover, PI matrix and silica nanoparticles both have alkyl groups which may enhance the interfacial interaction between two phases through nonpolar interactions. For the evaluation of property enhancement and comparative study, a series of PI-SiO₂ composites (OI-UM) was also prepared where the unmodified silica network was dispersed into PI matrix and resulting composites lack in CTC between O-I components. The percentage of silica phase in both hybrid system (OI-M and OI-UM) was varied from 0-30 wt% and their properties were studied using appropriate analytical techniques.

Experimental

Materials

4-Hydroxybenzaldehyde (Merck, Germany), 1,4-dibromobutane (Merck, Germany), potassium carbonate (Merck, Germany), ethanol (Merck, Germany), hydrazine monohydrate (64-65 %, Sigma-Aldrich, USA), dimethylformamide (DMF, Merck, Germany), 4,4'-oxydianiline (ODA, 97 %, Sigma Aldrich, USA), pyromellitic dianhydride (PMDA, 99.2 %, Sigma-Aldrich, USA), dimethylacetamide (DMAc, 99.8 %, water content <0.005 %, Sigma-Aldrich, USA), tetraethoxysilane (TEOS, 97.5 %, Acros Organics, Fair Lawn, N J), and 3-aminopropyltriethoxysilane (APrTEOS, 95 %, ABCR GmbH & Co, Germany).

Synthesis

Synthesis of 1,4-*bis*[4-(hydrazonomethyl)phenoxy]butane (4-BHPB)

A novel and facile route was adopted for synthesis of 4-BHPB as given in Fig 1. Hydrazine hydrate (2.5 g, 50 mmol),

molecular sieves (5 g, 4 Å), and absolute methanol (15 mL) were stirred for 30 min under inert atmosphere at about 0-5 °C. Afterward, a solution of 4,4'-(Butane-1,4-diylbis(oxy))dibenzaldehyde^{35, 36} (1 mmol) in methanol (10 mL) was added slowly to reaction flask. The reaction mixture was stirred at the same temperature for 8 hours. After complete consumption of the reactants, which was observed by TLC (chloroform: methanol, 9:1), the reaction mixture was cooled to room temperature. Allowing the reaction mixture to stand for 1 hour resulted in the precipitation of crude product which was retrieved by filtration. The dried product was re-dissolved in THF. The final product was precipitated by cooling the solution to 0 °C and was separated by filtration.

Yield: 78%. m.p 262-263 °C; FTIR: ν (cm⁻¹) 3387, 3347 (NH₂), 2942, 2863 (-CH₂), 1623 (-CH=N). ¹H NMR (300 MHz, DMSO-d₆): δ ppm 7.65 (¹H, s, methine proton), 6.52 (4H, s, NH₂), 4.02 (4H, s, 5, 5'), 1.85 (4H, s, 6, 6'), 6.91-6.88 (4H, d, J = 8.7 Hz, 2, 2'), 7.41-7.38(4H, d, J = 8.7 Hz, 3, 3'); ¹³C NMR (75 MHz, DMSO-d₆): δ ppm 129.45 (1), 114.96 (2, 2'), 126.96 (3, 3'), 158.70 (4), 67.56 (5, 5'), 25.87 (6, 6') 139.17 (C=N). Anal. Calcd for C₁₈H₂₂N₄O₂: C, 66.24; H, 6.79; N, 17.17. found: C, 66.04; H, 6.45; N, 16.99.

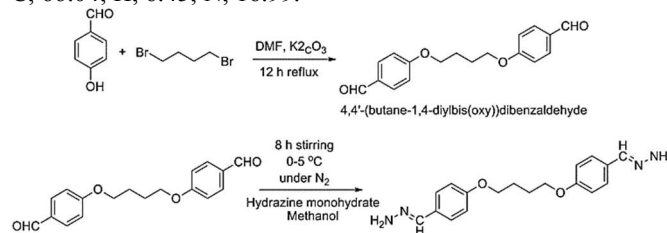


Fig 1 Synthesis of 1,4-*bis*[4-(hydrazonomethyl)phenoxy]butane (4-BHPB)

Synthesis of polyimide

High molecular weight PI was synthesized successfully by reacting diamine monomers (4-BHPB and ODA) with PMDA in a stoichiometric amount (Fig 2). 4-BHPB (1.55 g, 4.55 mmol) and ODA (8.37 g, 41.80 mmol) were dissolved in anhydrous DMAc (100 mL) by mechanically stirring the mixture for 1 h in a sealed glove box under inert and moisture free environment. After complete dissolution of both diamines in DMAc, PMDA (9.95 g, 45.61 mmol) was added in one portion with continuous stirring. With the advent of polymerization reaction, the viscosity of the solution was increased rapidly. In order to facilitate stirring, more DMAc was added to the solution. The polymerization reaction was carried out under the complete anhydrous conditions at about 5 °C. In order to ensure anhydrides as chain-end-groups instead of amino groups and compensate any lost anhydride functional group, dianhydride was added further (1% of initial weight) after stirring the polymer solution for 6 h. The reaction mixture was kept on stirring under the same conditions for 18 h in order to complete the polymerization reaction.

Afterwards, the solvent elution technique was used to cast PAA films which were thermally imidized into PI by successive heating at 100 °C, 200 °C, and 300 °C each for 1 h.

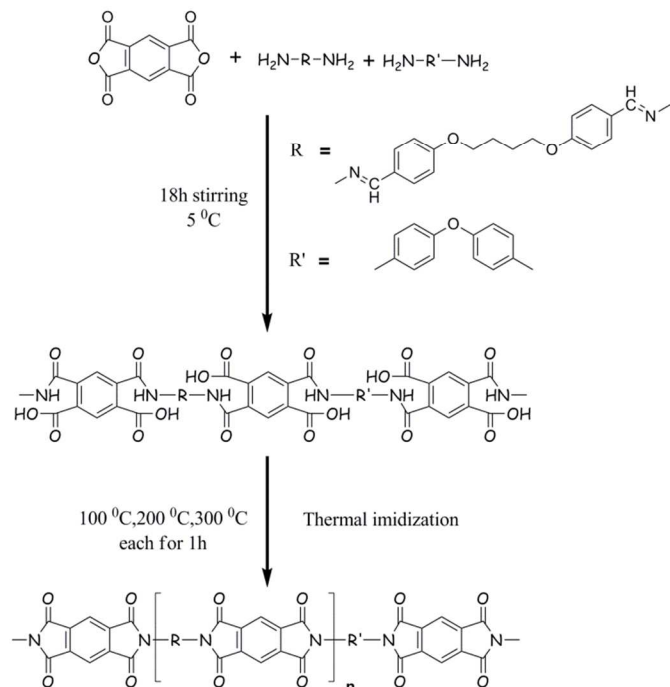
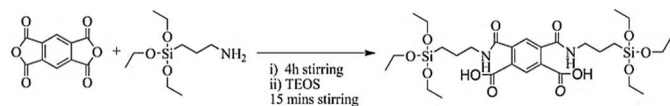


Fig 2 Synthesis of PI

Modification of silica nanoparticles

SiO₂ network was modified organically for increasing interphase compatibility and uniform dispersion of nanoparticles into PI matrix (Fig 3). This goal was achieved by preparing 2,6-bis(3-(triethoxysilyl)propyl)pyrrolo[3,4-f]isindole-1,3,5,7(2H,6H)-tetraone⁷ (M-SiO₂) by stirring APrTEOS and PMDA (2:1) in DMAc for 4 h. Subsequently, an appropriate amount of TEOS (40 % solution in DMAc) was added and oligomeric solution was stirred further for 1 h.

Fig 3 Synthesis of M-SiO₂**Synthesis of PI-SiO₂ composites**

Two types of O-I hybrids were prepared as discussed below.

Synthesis of polyimide-unmodified SiO₂ composite (OI-UM)

In OI-UM hybrid system, unmodified silica micro-particles were dispersed in situ in PI matrix. An appropriate amount of TEOS (40wt% solution in DMAc) was added to the PAA solution as given in Table 1. The reaction mixture was stirred for 1 h followed by the addition of acidified water. The temperature of the reaction mixture was raised to 60 °C followed by stirring for another 6 h. Afterwards, the reaction mixture was transferred to Teflon petri dishes and heated at 70 °C for 12 h to cast OI-UM hybrid films. The resultant flexible films were imidized thermally at 100 °C, 200 °C, and 300 °C each for 1 hour.

Synthesis of polyimide-modified SiO₂ composite (OI-M)

OI-M hybrid system was prepared by in situ generation of modified silica nanoparticles. A mixture of M-SiO₂, PAA solution, and acidified water was subjected to sol-gel reaction. Later, the solvent elution technique and thermal imidization process were exercised to cast and imidized hybrid films respectively as discussed earlier.

0-30 wt% SiO₂ was incorporated into the PI matrix (both in OI-UM and OI-M) via sol-gel reaction. Table 1 presents the

compositions and codes of hybrid films of OI-M and OI-UM composites.

Table 1 Compositions of PI-SiO₂ hybrid films

PI-SiO ₂ composites	Codes	M-SiO ₂ : TEOS (%)	Film composition		Film
			PI (wt %)	SiO ₂ (wt%)	
Pristine PI	0-PI	00:00	100	0	F, T
OI-UM					
	10UM	0:1	90	10	F, O
	20UM	0:1	80	20	F, O
	30UM	0:1	70	30	F, O
OI-M					
	10M	0.05:0.95	90	10	F, T
	20M	0.05:0.95	80	20	F, T
	30M	0.05:0.95	70	30	F, T

F = flexible, T = transparent, O = opaque

Characterization**FTIR Spectroscopy**

FTIR spectroscopy was employed to evaluate the structure of diamine monomer, nature of silica network, and conversion of PAA into PI. The FTIR spectra of all the species were recorded in the range of 4000-400 cm⁻¹ on a Perkin-Elmer FTIR 2000 spectrometer.

NMR Spectroscopy**¹H and ¹³C NMR spectroscopy**

Structures and purity of the synthesized monomer were elucidated by ¹H and ¹³C NMR spectroscopy. Bruker AM-300 spectrophotometer was used to record ¹H and ¹³C NMR spectra at 300 MHz and 75 MHz respectively.

Solid state ²⁹Si NMR Spectroscopy

The ²⁹Si NMR spectra, recorded on Bruker Avance 400WB NMR Spectrometer, were used to investigate the structure of organically modified silica network. The hybrid films were ground to powder form in freeze drier. Various silicate nuclei were differentiated from each other using very facile nomenclature. The silicate species having one organic side group were denoted by letter "T". "Q" were used to denote those species which do not have any organic side group, whereas "i" stands for the number of -O-Si groups directly bonded to Si atom.

Field emission scanning electron microscopy (FE-SEM)

The surface morphology of both OI-M and OI-UM hybrid films was studied using field emission scanning electron microscope S-4800. Flexible composite films were dipped in liquid nitrogen and then were cryo-fractured. Before examining, the samples were sputter-coated with platinum and vaulted on aluminium holders with the help of carbon tape. Secondary electron images were collected with a beam voltage of 10 keV using in-lens detector.

Atomic force microscopy (AFM)

Surface roughness analysis of hybrid films was carried out with the help of multimode digital instruments DI 3100 Nanoman AFM, Veeco Metrology, LLC, USA. Scanning probe microscopy (triangular cantilever containing a pyramidal tip made of silicon nitride) software WSxM 3.0 Beta v. 8.1 was utilized to capture AFM micrographs in tapping-mode under ambient conditions.

Contact angle measurements

The contact angle of pristine PI, OI-M, and OI-UM composites was analyzed on Phoenix 300 Plus, SEO Co, Ltd Contact Angle Analyzer using deionized water as providing liquid.

Thermogravimetric analysis (TGA)

TGA analysis at TG 209 F3, NETZSCH Germany, was used to access the thermal stability of neat PI and its silica reinforced composites. The vacuum dried samples were analyzed at a heating rate of 10 °C/min from 30 to 800 °C in an inert atmosphere of nitrogen.

Results and discussion

Monomer synthesis

Fig 1 presents the synthesis of 1,4-bis[4-(hydrazonomethyl)phenoxy]butane (4-BHPB) which comprises of two steps. The first step includes synthesis of 4,4'-(Ethane-1,2-diylbis(oxy))dibenzaldehyde by the nucleophilic substitution reaction of 4-hydroxybenzaldehyde with dibromoethane. Whereas, in the second step condensation reaction between 4,4'-(Ethane-1,2-diylbis(oxy))dibenzaldehyde and hydrazine monohydrate resulted in the preparation of 4-BHPB. Purity and structure of the synthesized product were comprehensively confirmed by FTIR, elemental analysis, ^1H and ^{13}C NMR spectroscopic techniques.

In the FTIR spectra, the diagnostic absorption band, attributed to $-\text{C}=\text{N}$, was observed at 1623 cm^{-1} . The absorption bands observed at 3387 cm^{-1} and 3347 cm^{-1} were assigned to asymmetric and symmetric stretching vibrations respectively of the amino group. Similarly, the para-substitution pattern of the benzene ring in the product was confirmed by an absorption band at 820 cm^{-1} .

The structure of 4-BHPB was further evaluated by the ^1H NMR spectroscopy where a singlet of two protons at 7.65 ppm, assigned to the protons of azomethine groups, confirmed the successful formation of the product (Fig 4). Four protons of amino group resonated at 6.52 ppm as singlet in the spectrum. In the aliphatic region, the four protons of methylene groups (5, 5') bonded to oxygen atom resonated at 4.02 ppm while protons of the central methylene groups (6, 6') appeared at 1.85 ppm.

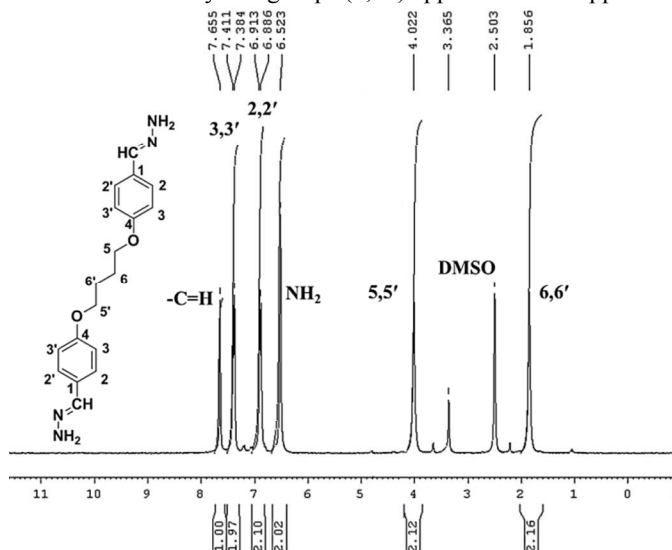


Fig 4 ^1H NMR spectrum of 4-BHPB

Further confirmation about the structure of 4-BHPB was derived from the ^{13}C NMR spectrum (Fig 5) where the peak for carbon atom of azomethine group was observed at 139.17 ppm. Thus,

the NMR data confirmed that the structure of 4-BHPB agreed with the proposed molecular structure.

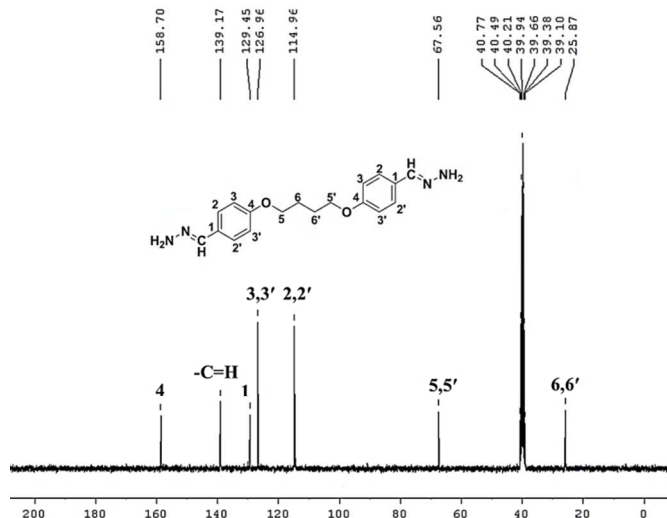


Fig 5 ^{13}C NMR spectrum of 4-BHPB

Characterization of polyimide-SiO₂ composites

Spectroscopic analysis

FTIR spectroscopy

FTIR spectroscopy was used to analyze the conversion of monomers into PAA, and PAA into PI.

FTIR spectrum of PI (Fig 6) shows that an absorption band at around 1650 cm^{-1} (characteristic of amide carbonyl group in PAA) disappeared. So, the presence of silica network imposed no detrimental effect on PI curing which is in good agreement with the previously published reports^{21, 37}. Conversion of PAA into PI was further supported by the presence of characteristic absorption band for asymmetric and symmetric stretching vibration of carbonyl groups (1759 cm^{-1} , 1720 cm^{-1} respectively), C-N stretching vibration (1360 cm^{-1}), and imide ring deformation (722 cm^{-1}).

In the FTIR spectra of OI-M and OI-UM hybrid system, a broad absorption band around $1100\text{--}1020\text{ cm}^{-1}$ is present, the intensity of this broad absorption band was observed to increase as the silica contents increased from 10-30 wt%. This absorption band appeared due to stretching vibrations of Si-O-Si linkages in the silica network³⁷. Moreover, it is also evident from Fig 6 that the height of this band was smaller and located at lower wave numbers in case of OI-M system as compared to the OI-UM system. Thus, it may be inferred that in OI-UM hybrid system the structure of silica network is dense and cyclic as compared to OI-M hybrid system where more open silica networks prevailed due to preceding chemical modification³⁷.

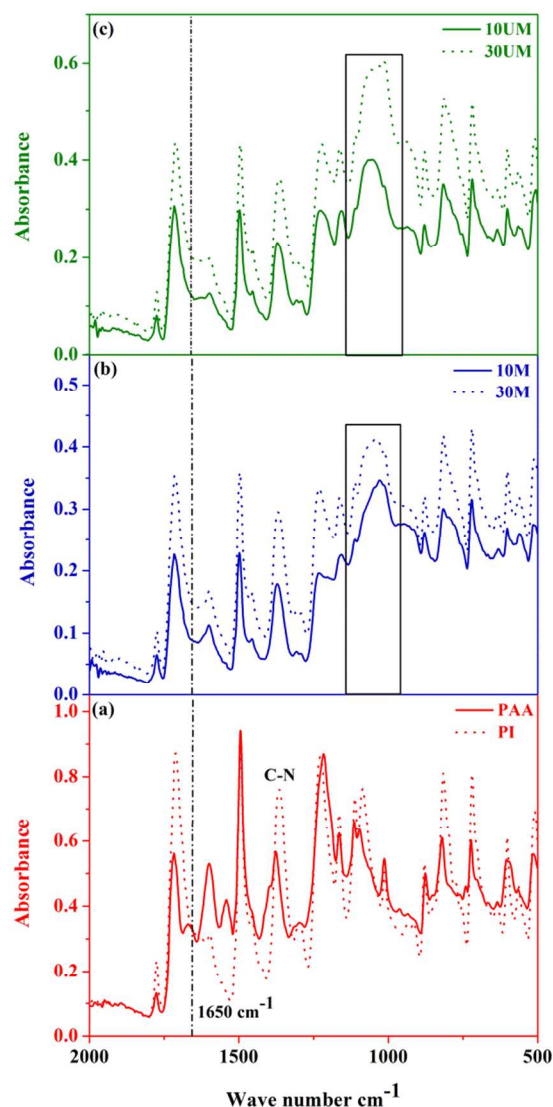


Fig 6 FTIR Spectra of PI and PI-SiO₂ hybrids: (a) PI, PAA (b) OI-M hybrids (c) OI-UM hybrids

Solid-state ²⁹Si NMR spectroscopy

²⁹Si NMR spectroscopy was used to evaluate the structure of silica network and to investigate the bonding environment of silicate nuclei. ²⁹Si NMR spectrum was recorded using cross polarization magic angle spinning (CP-MAS) technique with a relaxation delay of 3 s. Fig 7 presents the ²⁹Si NMR spectrum of 10M from OI-M hybrid system. Silica network in the OI-M hybrid system was comprised of four different types of silicate nuclei i.e Si(OSi)₄ (Q4) at -110 ppm, Si(OSi)₃(OH) (Q3) at -100 ppm, Si(OSi)₂OH₂ (Q2) at -91 ppm, and (SiO)₃Si-C (T) at -65 ppm. These chemical shift values are in accordance with the published literature³⁸⁻⁴⁰. The resonance peak corresponding to (SiO)₃Si-C nuclei (T) exhibits the successful organic modification of silica phase in OI-M hybrid system^{9, 38, 39}. The organic modification of silica nanoparticles resulted in uniform dispersion of particles in PI matrix and controlling the phase segregation between O-I component imparting the advanced properties to OI-M hybrid films.

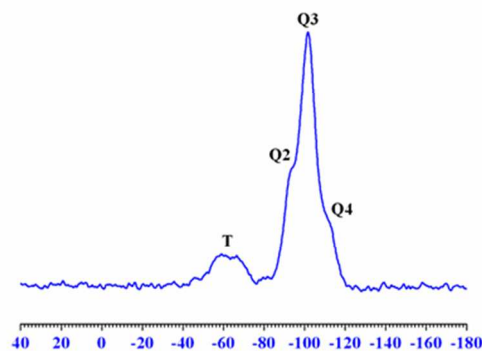


Fig 7 Solid-state ²⁹Si NMR spectrum of 10M

Microstructural analysis

a) FE-SEM

The FE-SEM micrographs in Fig 8 (a-d) for both OI-M and OI-UM hybrid systems (reinforced with 10 and 20 wt% silica) illustrate the influence of organic modification of the silica precursor. In OI-UM hybrid system (Fig 8a, and 8c) silica micro-beads (1-2 μm) have clear sharp boundaries and smooth surfaces. Wide gaps between PI matrix and silica micro-particles expose the weak interfacial interaction between O-I components. Such phase separation and thermodynamic immiscibility between O-I components are liable to act as stress concentration defect rather than competent reinforcement materials³¹. On the contrary, silica nanoparticles (30-40 nm) are appearing co-continuous and finely mixed with PI matrix in OI-M nanocomposites (Fig 8b, 8d). An improved interfacial interaction brought about a morphological transformation from a dispersed particle microstructure to finely interconnected and co-continuous phase morphology. An enhanced compatibility between O-I phases through the CTC and nonpolar interactions (Fig 9) are credited for the uniform dispersion of silica nanoparticles into PI matrix.

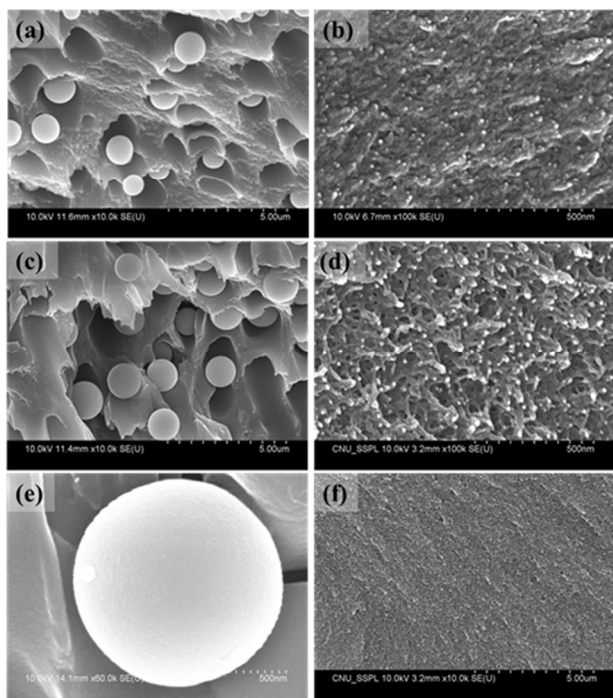


Fig 8 FE-SEM micrographs (a) 10UM, (b) 10M, (c) 20UM, (d) 20M (e) 20UM at 500 nm, (f) 20M at 5 μm

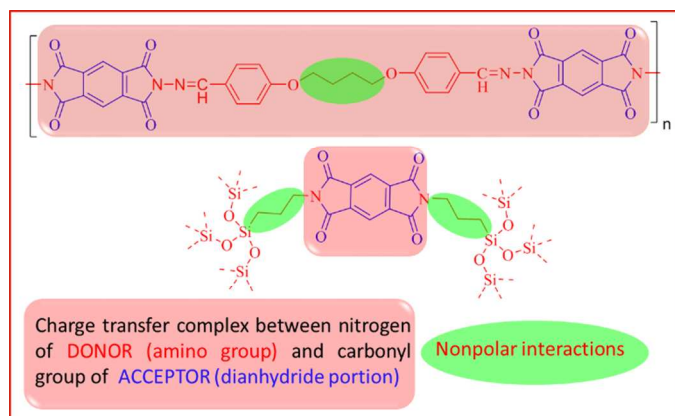


Fig 9 Charge transfer complex and nonpolar interactions between PI chains and silica nanoparticles

b) Atomic force microscopy (AFM)

AFM was used to study the surface roughness and morphology of the OI-UM and OI-M composite systems. Fig 10 (a-d) illustrates the two- and three-dimensional AFM micrographs of both types of PI-SiO₂ hybrids. It is obvious from micrographs (Fig 10a and 10b) that the surface of the OI-UM hybrid system is occupied with contours of different sizes. The values of root mean square roughness (Rq) and average roughness (Ra) were found to be 3.82 nm and 4.37 nm respectively. In comparison, OI-M hybrid films (Fig 10c and 10d), due to efficient dispersion of silica nanoparticles, exhibited much uniform and smooth surface with Rq and Ra values as low as 0.42 nm and 0.33 nm respectively. It can be concluded that the uniformity and planarity of the OI-M hybrid films are significantly enhanced as compared to hybrid films of the OI-UM system.

Inserting Graphics

Graphics should be inserted where they are first mentioned (unless they are equations, which appear in the flow of the text). They can be single column or double column as appropriate.

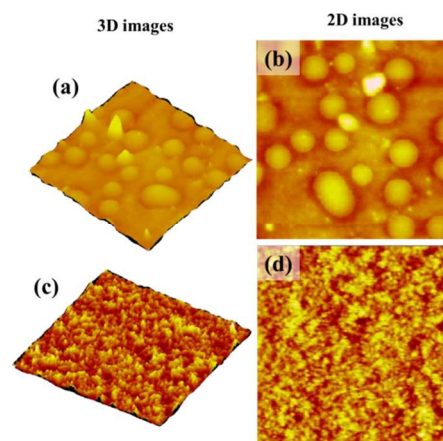


Fig 10 AFM micrographs ($3 \times 3 \mu\text{m}$) of (a, b) 3D and 2D images of OI-UM hybrid system (c, d) 3D and 2D images of OI-M hybrid system

Contact angle measurement

Contact angle analysis furnishes useful information about the hydrophobicity or hydrophilicity of the surface of the polymer materials. Hydrophobic surfaces have contact angles in the range of about 70° to 90° while hydrophilic surfaces have low values (0-30°)⁴¹. The values of contact angle (θ) for OI-M and OI-UM systems are given in Table 2. The variations in the contact angle as a function of silica contents are shown in Fig 11. In the case of the OI-M, integration of silica nanoparticles into the PI matrix lead to an increase in the contact angle values from 65.5° for the pristine PI to 93.3° at 30 wt% silica loading. On the other hand, this value increased to 83.2° in the case of OI-UM hybrid at 30wt% silica content.

Thus, OI-M hybrid films were found more hydrophobic with an increase of 27.8° in contact angle values (0 to 30 wt %) as compared to OI-UM hybrid films which exhibit an increment of 17.7°. Higher values of contact angle and enhanced hydrophobicity of the OI-M system as compared to OI-UM system may be attributed to nonpolar interactions of alkyl groups and CTC as a result of electron donor and electron acceptor groups present together in O-I phases. Enhanced hydrophobicity of PI-SiO₂ coatings prevent the infusion of water to the substrate (e.g. metal and/or ceramics), thereby minimizing the chances of deterioration of coating⁴².

Table 2 Values of contact angles of PI-SiO₂ hybrids

Codes	Contact angle (θ)
0-PI	65.5
OI-UM	
10UM	74.9
20UM	79.2
30UM	83.2
OI-M	
10M	79.6
20M	87.3
30M	93.3

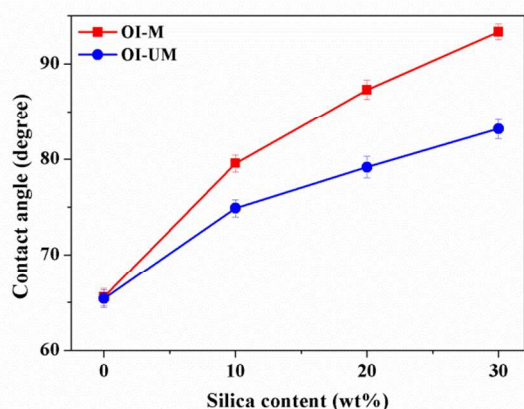


Fig 11 Comparison of contact angle of the OI-M and OI-UM hybrid systems as a function of silica content

Thermal properties

The effect of improved miscibility of PI matrix with silica nanoparticles through CTC on the thermal properties of resulting hybrid films was evaluated using the thermogravimetric analysis. The hybrid films were analyzed at a heating rate of 10 °C/min in the inert atmosphere of nitrogen. Fig 12 shows the TGA thermograms of both hybrid systems reinforced with 10-30 wt% silica phase, whereas Table 3 gives some derived data. The thermal stability of the hybrids was assessed in terms of temperatures at 10 % weight loss (T_{10}), and residual mass at 800 °C. Table 3 shows that the value of thermal decomposition temperature T_{10} is 558 °C for pristine PI, while it was 20 °C higher for OI-UM and 34 °C higher for OI-M hybrid system at 30 wt% silica content as compared to pristine PI. A comparison of the thermal stability among the both hybrid systems exhibited that modified silica nanoparticles raised the values of T_{10} to a greater extent as compared to the unmodified silica networks. Similarly, the residual mass at 800°C has higher values for OI-M hybrid system as compared to OI-UM system. The delayed decomposition process of the PI matrix revealed that incorporation of modified silica nanoparticles resisted the diffusion of oxygen into the PI matrix

and consequently reduced the degradation at elevated temperature³¹. In contrast to the unmodified silica particles, the modified silica phase was well adhered and well mixed to the matrix. The existence of CTC due to electron donor-acceptor groups and nonpolar interactions due to alkyl groups present simultaneously in O-I phases makes organically modified silica nanoparticles effective heat and mass transport barrier, and hence conserved the matrix more efficiently.

Table 3 Thermal properties of pristine PI and PI-SiO₂ hybrids

Codes	T_{10} (°C)	Residual mass (wt%)
0-PI	558	25
OI-M		
10M	569	33
20M	580	41
30M	592	49
OI-UM		
10UM	563	30
20UM	570	36
30UM	578	43

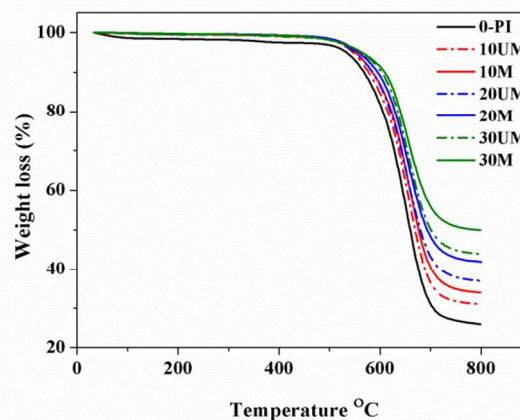


Fig 12 Comparison of thermal stability of OI-M and OI-UM hybrid systems

Conclusions

The charge transfer complex (through novel diamine 4-BHPB in PI matrix and M-SiO₂ in silica nanoparticles) as well as nonpolar interaction between the alkyl groups of O-I components significantly raised the compatibility between PI matrix and nano-scale silica phase. The presence of different types of silicate nuclei and organic modification of silica domain was investigated by solid state ²⁹Si NMR spectroscopy. FE-SEM micrographs revealed that M-SiO₂ led to controlled particle size (below 50 nm), much reduced agglomeration, and uniform dispersion of silica nanoparticles into the PI matrix in

case of OI-M hybrids. In comparison, OI-UM hybrids displayed silica micro-beads completely detached from the PI matrix with particle size ranging between 1-2 μm . Similarly, OI-M hybrid films were found more hydrophobic as compared to OI-UM hybrid films. Thermal stability exhibited the similar trend, i.e. values of T_{10} and residual mass at 800 $^{\circ}\text{C}$ remained always higher for OI-M hybrid system as compared to OI-UM hybrid system. Thus, it can be inferred that CTC between O-I phases presented a remarkable enhancement to the eventual properties of OI-M hybrid system by ensuring efficient dispersion of silica nanoparticles, strengthening interfacial interactions, and inhibiting phase segregation.

Notes and references

^a Department of Chemical and Biomolecular Engineering, KAIST, 291 Daehak-ro, Yuseong-gu, Daejeon 305-701, Republic of Korea.

^b Department of Chemistry, Quaid-i-Azam University, Islamabad 45320, Pakistan.

^c Department of Metallurgy and Materials Engineering, Pakistan Institute of Engineering and Applied Sciences (PIEAS), Islamabad 45650, Pakistan.

^d Department of Liberal Arts and Sciences, Virginia Commonwealth University in Qatar, PO Box 8095, Doha, Qatar.

† Footnotes should appear here. These might include comments relevant to but not central to the matter under discussion, limited experimental and spectral data, and crystallographic data.

Electronic Supplementary Information (ESI) available: [details of any supplementary information available should be included here]. See DOI: 10.1039/b000000x/

- M. Miki, T. Suzuki and Y. Yamada, *Journal of Applied Polymer Science*, 2013, **130**, 54-62.
- T. Suzuki and Y. Yamada, *Journal of Applied Polymer Science*, 2013, **127**, 316-322.
- T. Akhter, S. Saeed, H. Siddiqi, O. O. Park and G. Ali, *J Polym Res*, 2013, **21**, 1-11.
- A. Romero, M. Parentis, A. Habert and E. Gonzo, *J Mater Sci*, 2011, **46**, 4701-4709.
- D.-J. Liaw, K.-L. Wang, Y.-C. Huang, K.-R. Lee, J.-Y. Lai and C.-S. Ha, *Progress in Polymer Science*, 2012, **37**, 907-974.
- T. Akhter, S. Saeed, H. M. Siddiqi and O. Ok Park, *Polymers for Advanced Technologies*, 2013, **24**, 407-414.
- T. Akhter, H. Siddiqi, S. Saeed, O. O. Park and S. Mun, *J Polym Res*, 2014, **21**, 1-10.
- X. Wang, L. Wang, Q. Su and J. Zheng, *Composites Science and Technology*, 2013, **89**, 52-60.
- L. Zou, S. Roddecha and M. Anthamatten, *Polymer*, 2009, **50**, 3136-3144.
- P. Musto, G. Ragosta, G. Scarinzi and L. Mascia, *Polymer*, 2004, **45**, 1697-1706.
- M. Nandi, J. A. Conklin, L. Salvati and A. Sen, *Chemistry of materials*, 1991, **3**, 201-206.
- P. Musto, M. Abbate, M. Lavorgna, G. Ragosta and G. Scarinzi, *Polymer*, 2006, **47**, 6172-6186.
- Y. Li, G. He, S. Wang, S. Yu, F. Pan, H. Wu and Z. Jiang, *Journal of Materials Chemistry A*, 2013, **1**, 10058-10077.
- G. Kickelbick, *Progress in polymer science*, 2003, **28**, 83-114.
- G. Ragosta, P. Musto, M. Abbate and G. Scarinzi, *Journal of applied polymer science*, 2011, **121**, 2168-2186.
- A. Morikawa, H. Yamaguchi, M. Kakimoto and Y. Imai, *Chemistry of materials*, 1994, **6**, 913-917.
- Z. Ahmad and J. E. Mark, *Chemistry of materials*, 2001, **13**, 3320-3330.
- H. Zou, S. Wu and J. Shen, *Chemical reviews*, 2008, **108**, 3893-3957.
- Y. Deng, M. Wu, X. Liu and Y. Gu, *European Polymer Journal*, 2010, **46**, 2255-2260.
- C. Kizilkaya, S. Karataş, N.-K. Apohan and A. Güngör, *Journal of Applied Polymer Science*, 2010, **115**, 3256-3264.
- S. Saeed, M. Khalil and Z. Ahmad, *Journal of Macromolecular Science, Part A*, 2009, **46**, 152-162.
- S. Sinha Ray and M. Okamoto, *Progress in Polymer Science*, 2003, **28**, 1539-1641.
- C. J. Cornelius and E. Marand, *Journal of membrane science*, **2002**, **202**, 97-118.
- C. J. Cornelius and E. Marand, *Polymer*, 2002, **43**, 2385-2400.
- S. H. Wang, Z. Ahmad and J. E. Mark, *Chemistry of materials*, 1994, **6**, 943-946.
- L. Mascia and A. Kioul, *Polymer*, **1995**, **36**, 3649-3659.
- S. Al-Kandary, A. A. M. Ali and Z. Ahmad, *Journal of material science*, 2006, **41**, 2907-2914.
- S. Al-Kandary, A. A. M. Ali and Z. Ahmad, *Journal of applied polymer science*, 2005, **98**, 2521-2531.
- C. Joly, M. Smahi, L. Porcar and R. D. Noble, *Chemistry of materials*, 1999, **11**, 2331-2338.
- J. W. Gilman, C. L. Jackson, A. B. Morgan, R. Harris, E. Manias, E. P. Giannelis, M. Wuthenow, D. Hilton and S. H. Phillips, *Chemistry of Materials*, 2000, **12**, 1866-1873.
- M. Khalil, S. Saeed and Z. Ahmad, *Journal of Applied Polymer Science*, 2008, **107**, 1257-1268.
- B. V. Kotov, T. A. Gordina, V. S. Voishchev, O. V. Kolniov and A. N. Pravednikov, *Polymer Science U.S.S.R.*, 1977, **19**, 711-716.
- M. Nishihara, L. Christiani, A. Staykov and K. Sasaki, *Journal of Polymer Science Part B: Polymer Physics*, 2014, **52**, 293-298.
- J. Ferraris, D. O. Cowan, V. Walatka and J. H. Perlstein, *Journal of the American Chemical Society*, 1973, **95**, 948-949.
- K. Balaji and S. C. Murugavel, *Journal of polymer science part A: polymer chemistry*, **2011**, **49**, 4809-4819.
- A. Tabbusum, Quaid-i-Azam University, Islamabad 45320, Pakistan, 2012.
- W. Stober, A. Fink and E. Bohn, *J. Colloid Interface. Sci*, **1968**, **26**, 62-69.
- Y. Gao, N. R. Choudhury, N. Dutta, J. Matisons, M. Reading and L. Delmotte, *Chemistry of materials*, 2001, **13**, 3644-3652.
- V. Moravetski, J. R. Hill, U. Eichler, A. K. Cheetham and J. Sauer, *Journal of American chemical society*, 1996, **118**, 13015-13020.
- D. H. Gray, S. Hu, E. Juang and D. L. Gin, *Advanced materials*, 1997, **9**, 731-736.
- C. J. Chen, H. T. Lu, W. Y. Tseng, I. H. Tseng, S. L. Huang and M. H. Tsai, *Journal of applied polymer science*, 2011, **122**, 648-656.

42. Y. Chen and J. O. Iroh, *Chemistry of materials*, 1999, **11**, 1218-1222.